J Wood Sci (2011) 57:371–376
DOI 10.1007/s10086-011-1187-9

ORIGINAL ARTICLE

Ken Watanabe · Satoshi Shida · Masamitsu Ohta

Evaluation of end-check propagation based on mode I fracture toughness of sugi (*Cryptomeria japonica*)

Received: April 12, 2010 / Accepted: March 9, 2011 / Published online: June 28, 2011

Abstract The relation between crack propagation based on fracture mechanics and end-check propagation during drying was evaluated in this study. Corresponding to the direction of end-check propagation, the mode I fracture toughness of air-dried sugi specimens in TR, TL, and intermediate systems was examined by single-edge-notched bending tests. The occurrence and propagation of end checks on sugi (*Cryptomeria japonica* D. Don) blocks during drying were observed at the scale of the annual rings. It was found that the critical stress intensity factor (K_{IC}) decreased as the crack propagation changed from TL to TR. The value of K_{IC} in the TR system was significantly lower than that in the TL system. As a measure of fracture energy, the area under the load–crack opening displacement curve in the TR system was more than twice that in the TL and intermediate systems. These results indicate that cracks perpendicular to the tangential direction initiate radially with ease, and then crack arrest occurs to prevent growing. This finding provides a consistent interpretation of the end-check propagation observed during drying as follows: tiny end checks, as an analog of TR cracks, occur easily and selectively in latewood or transition wood and propagate toward the pith during drying. When there is no corresponding secondary check in the forward latewood, the checks are arrested and do not propagate further.

Key words Fracture toughness · TR and TL systems · End check · Occurrence and propagation · Sugi · Drying

K. Watanabe (✉)
Forestry and Forest Products Research Institute, 1 Matsunosato, Tsukuba, Ibaraki 305-8687, Japan
Tel. +81-29-829-8306; Fax +81-29-874-3720
e-mail: kenwatanabe@ffpri.affrc.go.jp

S. Shida · M. Ohta
Department of Biomaterials Science, University of Tokyo, Tokyo 113-8657, Japan

Introduction

Driven by the significant value loss due to surface checks that occur on side-grain surfaces during lumber processing, interest has arisen in the investigation of drying stresses associated with surface checks over the past decades. At the beginning of drying, end checks, which are similar to surface checks but appear on the ends of lumber, occur easily and develop into severe defects, such as splits. The occurrence of end checks can be explained by rapid longitudinal moisture movement which results in high stresses in the lumber ends due to quick drying.[1] Without end-coating, even if the lumber is stacked indoors under cyclically varying relative humidity where the drying stress is assumed to be much smaller than the failure stress, it is inevitable that end checks will develop. Thus, the traditional explanation based on stress-based failure criteria is insufficient to explicate the occurrence of end checks.

Independent of the drying conditions, the occurrence and propagation of end checks have a specific pattern in most softwood species. For example, sugi (*Cryptomeria japonica*) lumber is exposed to cyclically varying relative humidity conditions, and some end checks occur across latewood end-grain surfaces (Fig. 1a). The short inner end checks do not tend to propagate. Later, end checks occur on the edge of the end-grain surface (Fig. 1b), and these propagate straightforwardly in the longitudinal direction and develop into long surface checks (Fig. 1c). Rather than material mechanics, fracture mechanics is considered to be more suitable for describing the mechanism of the occurrence and propagation of end checks.

It is well known that the damage of wood fibers in both end-grain and side-grain surfaces is caused by machining of wood, e.g., sawing, planning, and sanding.[2–4] Stehr investigated the sawn end-grain and planed side-grain surfaces of softwoods using scanning electron microscopy.[4] The crushed and damaged surfaces that can be expected to contain failure initiation sites in terms of wood adhesion were observed in both end-grain and side-grain surfaces. Stehr also pointed out that microscopic tip cracks occurred in sapwood of Scots pine

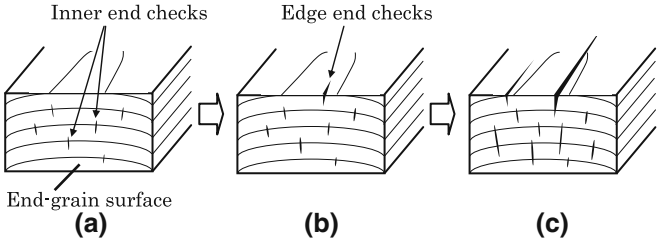

Fig. 1a–c. Specific pattern of end check occurrence and propagation on end grain of sugi lumber. Initially, inner end grain checks appear (**a**); later, edge end checks appear (**b**) and propagate longitudinally (**c**)

(*Pinus sylvestris*) after machining.[5] Therefore, it is assumed that these microscopic cracks after machining act as initiation sites of end checks, and start propagation.

In regard to drying checks, many studies have focused on the effects of parameters such as moisture content[6–10] and temperature[6,10,11] on mode I fracture toughness of wood. Sobue et al. investigated the influence of drying stress on the fracture toughness of European beech (*Fagus sylvatica*) in the TR system[12] The critical stress intensity factor (K_{IC}) decreased with the decrease of moisture content from approximately 80% to 30% during drying, and the decrease in K_{IC} was sensitive to the drying rate, demonstrating that the diminution of K_{IC} resulted from the residual drying stresses. Although the above findings have provided important information for understanding drying checks, few reports take into consideration the above mechanism of the occurrence and propagation of end checks or the difference between end and surface checks.

Due to the orthotropic nature of wood, mode I fracture toughness for different directions of crack propagation is expressed using the six principal crack-propagation systems. End checks occur perpendicular to the tangential direction and propagate along radial, longitudinal, and intermediate directions simultaneously, corresponding to TR, TL, and intermediate systems, respectively. Thus, it is important to evaluate fracture toughness not only for TR and TL cracks, but also for intermediate cracks. Nevertheless, no measure of the fracture toughness of intermediate cracks has been reported. This study was aimed at understanding the pattern of end-check occurrence and propagation at the scale of annual rings and at examining the mode I fracture toughness of sugi in TR, TL, and intermediate systems, which correspond to the direction of end-check propagation. The crack propagation for various directions from TR to TL systems was evaluated based on the obtained fracture toughness values and load–crack opening displacement (COD) curves.

Materials and methods

Specimens for single-edge-notched (SEN) bending tests

After being cut from a piece of sugi (*Cryptomeria japonica* D. Don) lumber, specimens with dimensions of $24 \times 24 \times 24$ mm^3

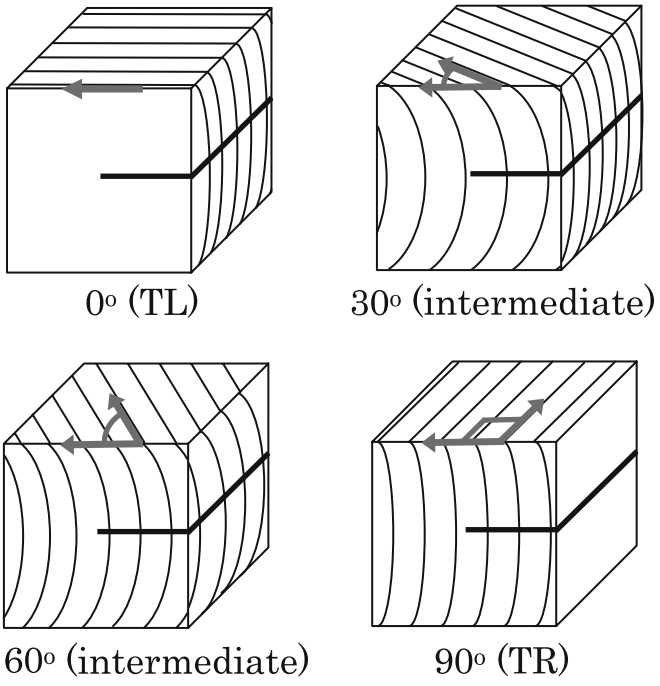

Fig. 2. TR, TL, and intermediate (30° and 60°) crack propagation systems of the specimens. The angles are between the L–T plane and the crack propagation direction

were conditioned at 20°C and 65% relative humidity before and during tests. The mean moisture content and density of the specimens were 9.8% and 0.40 g/cm^3, respectively. The specimens had four annual rings per 10 mm of radial length.

Using a thin band saw, a notch with a thickness of 1 mm was initially made to 10 mm depth and then extended 1 mm more by a razor blade. The notch direction was changed in accordance with the TR, TL, and intermediate systems, which correspond to the direction of end checks. Since the latewood layer was too narrow to maintain the notch tip in latewood for all replicates, the position of the notch tip in the annual ring was located in earlywood for the TR system.

Figure 2 illustrates the four types of crack propagation systems on the specimens. The angles between the direction of crack propagation and the L–T plane of 0° and 90° coincided with the TL and TR systems, respectively. The crack propagated from the bark side to the pith side, except for the TL system. With five replicates for each crack propagation system, four specimens were cut from the same annual rings and matched.

Each specimen was glued along the tangential direction of the specimen by epoxy resin adhesive to small pieces of wood (24×24 mm^2 in cross section and 43 mm length) that were obtained from the same piece of lumber, and then SEN specimens with dimensions of $24 \times 24 \times 110$ mm^3 were made (Fig. 3).

SEN bending tests

In three-point bending tests, SEN specimens were supported with a span of 96 mm, and a load was applied at the

center of the span with a crosshead speed of 1 mm/min using an Instron testing machine (Type 4204, Instron). COD was measured every second using a clip gauge and the critical stress intensity factor (K_{IC}) was calculated using the following equations:[13]

$$K_{IC} = \sigma_C \sqrt{\pi a} F\left(\frac{a}{W}\right) \quad (1)$$

$$\sigma_C = \frac{3SP_C}{2W^2} \quad (2)$$

$$F\left(\frac{a}{W}\right) = 1.090 - 1.735\left(\frac{a}{W}\right) + 8.20\left(\frac{a}{W}\right)^2 - 14.18\left(\frac{a}{W}\right)^3 + 14.57\left(\frac{a}{W}\right)^4 \quad (3)$$

where σ_c is the nominal critical stress, a is the notch length, W is the specimen width, S is the span length, P_c is the critical load for crack initiation per unit thickness, and $F\left(\frac{a}{W}\right)$ is the shape factor. Although, this formula was intended for isotropic materials, it was verified by finite element analysis that the application can be approximately extended to wood.[14,15]

Figure 4 shows the typical load–COD relationships of TR, TL, and intermediate systems. Crack initiation in the TL and intermediate systems was observed before reaching the maximum load (P_{max}) and after the proportional-limit load. On the other hand, the cracks in the TR system initiated with a slight snick when the load dropped before the proportional-limit load. Therefore, P_c was determined as the load at the intersection point between the load–COD curve and the straight line with a 5% reduction in initial slope (Fig. 4).

One-way analysis of variance (ANOVA) was conducted to test the differences of K_{IC} among the four crack propagation systems. Following one-way ANOVA, the Tukey-Kramer multiple comparison test was used to compare pairwise means.

Observation of end checks at the scale of annual rings

Five specimens cut perpendicular to the grain from a piece of heart-boxed square green sugi lumber were used for the observation of end checks. The specimens (with dimensions of 105 × 105 × 20 mm^3) were free of end checks and knots. The mean moisture content and density were 71.1% and 0.62 g/cm^3, respectively. After the specimens were placed in an oven at a temperature of 65°C, cross-sectional images were taken every 1 min using a commercial digital camera until the end checks stopped growing.

Results and discussion

Figure 5 shows the relationship between K_{IC} and the angle between the direction of crack propagation and the L–T plane. The value of K_{IC} decreased with increasing angle. The mean values of K_{IC} for 0° (TL) and 90° (TR) were 0.24 and

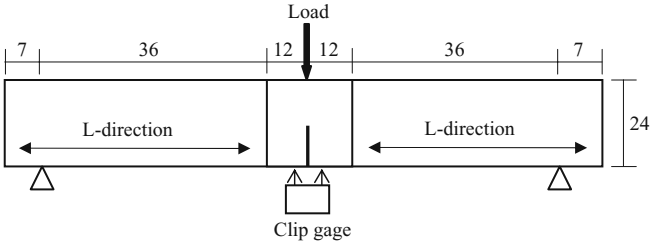

Fig. 3. Schematic of single-edge-notched (SEN) bending specimen. The units are given in millimeters

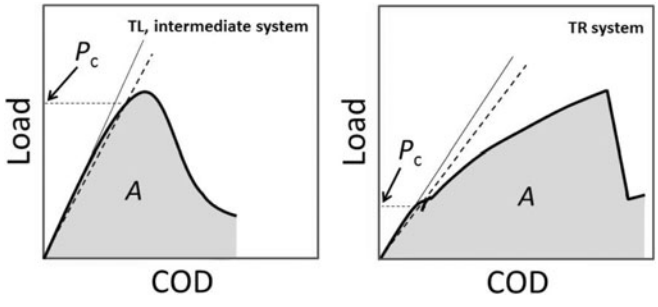

Fig. 4. Schematic load–crack opening displacement (COD) relationship of the TL and intermediate systems (*left*) and the TR system (*right*) obtained by SEN bending tests. The *solid line* indicates the initial slope, and the *dashed line* is the straight line with a 5% reduction in initial slope. The load–COD curve was depicted until the measurement just before the complete separation of the specimen. P_c, critical load for crack initiation per unit thickness; A, area under the curve

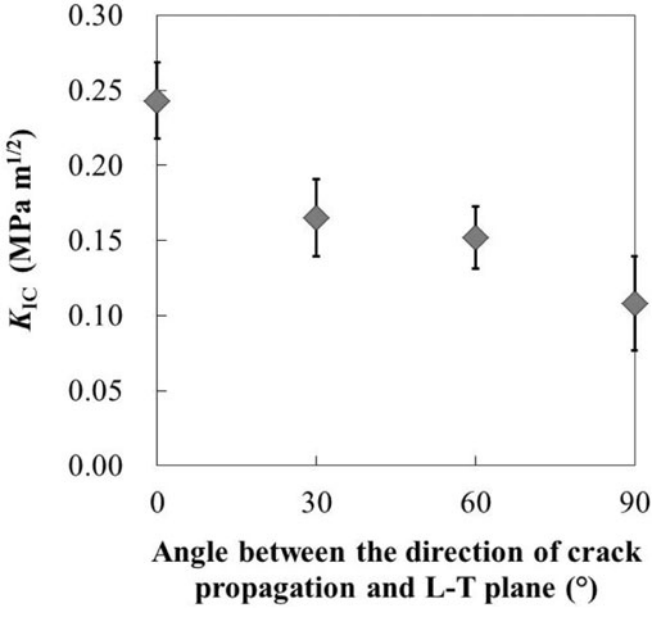

Fig. 5. Relationship between critical stress intensity factor (K_{IC}) and the angle between the direction of crack propagation and the L–T plane. The *plots* and the *error bars* indicate mean values and standard deviations, respectively

0.11 MPa $m^{1/2}$, respectively. Significant differences in K_{IC} were found at a 95% confidence level between all the different systems except for 30°–60° and 60°–90°. While Thuvander and Berglund[16] suggested that TR cracks are considered to show higher fracture toughness than TL cracks, the difference in fracture toughness between TR and TL systems was found to be variable in previous studies,[17–20] depending on the test methods, species used, and the definition of P_c. In this study, it is clear from the statistical analysis that the K_{IC} value in the TR system was significantly lower than that in the TL system (one-way ANOVA, $P < 0.01$; Tukey-Kramer multiple comparison test, $P < 0.01$), indicating that cracks perpendicular to the tangential direction initiate radially easier than they do longitudinally.

The intermediate system showed a higher K_{IC} than the TR system and a lower K_{IC} than the TL system. Since intermediate cracks intersect with annual rings obliquely, it is possible that the crack propagated obliquely to the notch direction, resulting in a nonuniform stress intensity distribution in the vicinity of the crack tip along the width of the SEN specimen. Therefore, it should be noted that the K_{IC} values for 30° and 60° obtained from Eqs. 1–3 are approximate. Maruyama and Okazaki[21] described the influence of the annual ring angle on mode I fracture toughness for a crack propagating perpendicular to the grain (LR and LT systems) using western hemlock (*Tsuga heterophylla*) and Douglas-fir (*Pseudotsuga taxifolia*). The critical strain energy release rate (G_{IC}) in the LR and LT systems was lower than G_{IC} in the intermediate systems. These results show that the influence of the annual ring angle on fracture toughness varies depending on the crack propagation perpendicular/parallel to grain. This variation of fracture toughness in intermediate systems may be ascribed to the nonuniformity of stress intensity distribution in the vicinity of the crack tip along the width of SEN specimens. Further finite element analyses will be required to validate this tentative theory.

Because of limitations on the specimen size and unstable crack propagation, a crack growth resistance curve (*R*-curve) could not be determined for all specimens. Thus, the properties of fracture mechanics were evaluated from the obtained load–COD curves. Figure 6 shows typical load–COD curves for the different crack propagation systems. The initial slope characterized the elastic properties and was proportional to the effective modulus of elasticity.[22] The initial slope of the TL specimen was much higher than that of the TR specimen. The intermediate specimens showed intermediate initial slopes between those of the TR and TL systems. This agrees with the known fact that the conventional modulus of elasticity is higher in the longitudinal direction than in the radial direction.

The load reached P_c at a COD of around 0.2 mm, when a drop of load with a slight decrease in COD was clearly observed in all TR specimens (Fig. 6). The load steadily increased with some slow crack growth, and then cracks were arrested when approaching the front of the latewood prior to the onset of brittle propagation. It is clear that P_c was reached and crack arrest in the TR system took place before P_{max} was reached. Stanzl-Tschegg reported similar

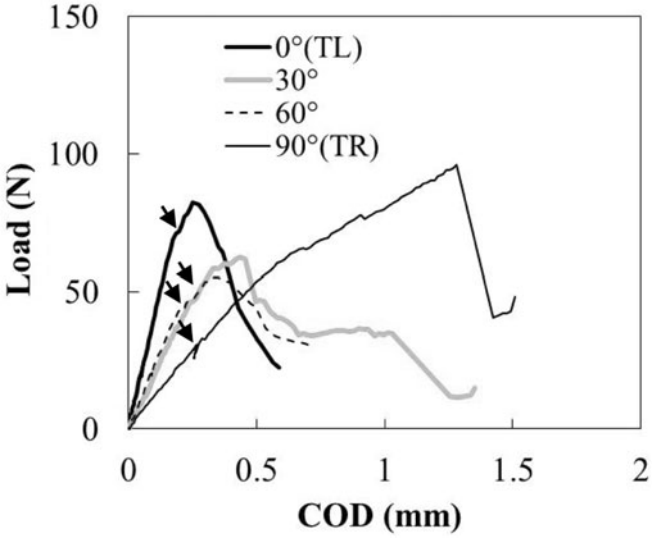

Fig. 6. Typical load–COD curves of TL (0°), TR (90°), and intermediate (30°, 60°) systems in the SEN bending tests. *Arrows* indicate P_c

behavior for the load–COD curve using spruce (*Picea abies*) specimens in a TR system,[23] demonstrating that fracturing in the increasing part of the load–displacement curve was mainly through cell walls, and that cracks usually changed their fracture planes during propagation at the scale of individual cells. In this study, on the other hand, the crack path of all specimens was nearly a straight line at the annual ring scale, and no kink crack was observed. In contrast, the load in the TL specimens increased rapidly and reached the P_{max}. More stable crack propagation after the P_{max} was shown, compared to the crack in the TR system. The load–COD curves of intermediate specimens depicted similar tendencies to that of the TL specimens.

The area under the entire load–COD curve in Fig. 4 is a measure of the fracture energy because it is the work required to grow cracks.[24] In the SEN bending tests, the load suddenly dropped with a large increase in COD at the moment the specimen completely separated. As a result, the COD at the moment of complete separation could not be measured accurately. Therefore, the area (A) up to the previous measurement before complete separation (Fig. 4) was calculated. Although it is possible that the indentation at loading point had an influence on the load–COD curve, we assume that A is useful for a relative comparison between different directions of crack propagation. The mean A value of the TR specimens was more than twice those of the other systems (Fig. 7), demonstrating that more energy was required to grow TR cracks than TL and intermediate cracks.

Figure 8 shows the typical pattern of the occurrence and propagation of end checks at the scale of annual rings. Although end checks on the end-grain surface developed in the radial, longitudinal, and intermediate directions simultaneously, only propagation in the radial direction, as an analog of the TR crack in the SEN bending tests, could be visually observed.

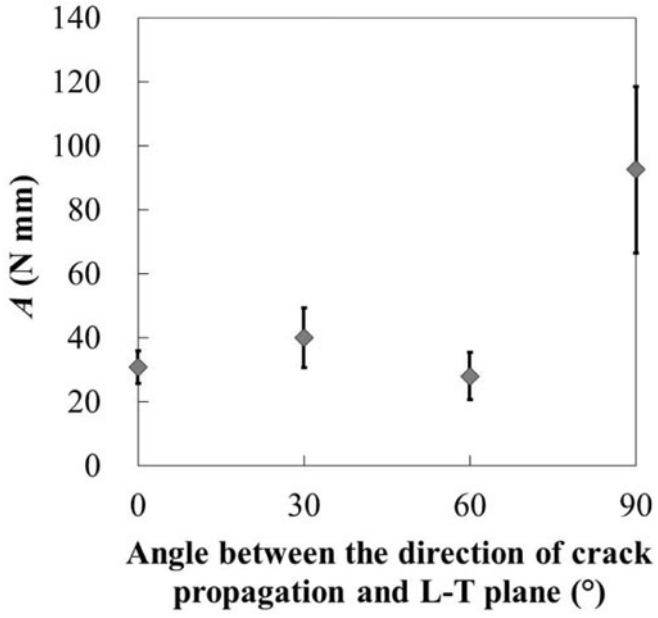

Fig. 7. Relationship between the area under the load–COD curve (A) and the angle between the direction of crack propagation and the L–T plane. The *plots* and the *error bars* indicate mean values and standard deviations, respectively

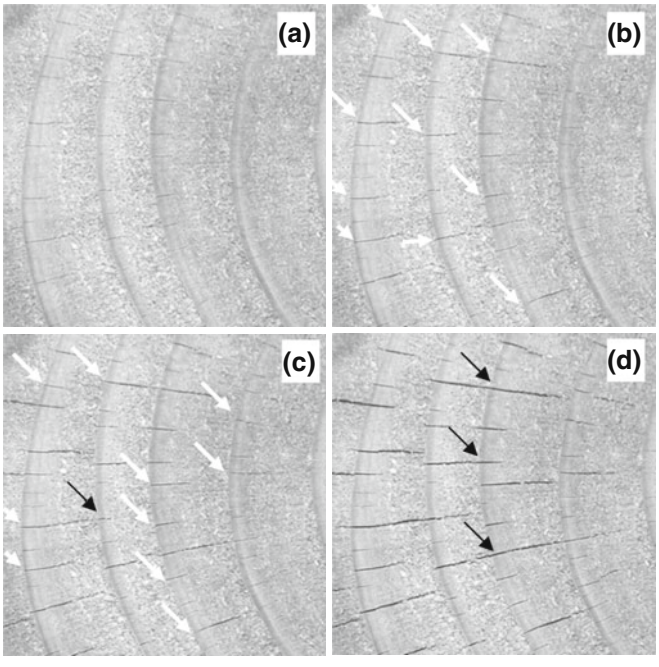

Fig. 8. Typical pattern of end-check occurrence and propagation of end checks during drying. **a**, **b**, **c**, and **d** are the views after 6, 7, 8, and 11 min of drying, respectively. *White* and *black arrows* indicate the halting of crack propagation and crack connection at the boundary between earlywood and latewood, respectively

First, tiny checks occurred not in the earlywood, but in the latewood or transition wood (Fig. 8a). Thuvander et al.[25] described the micromechanisms of radial crack growth. The latewood layer ahead of the crack tip carried a substantial tensile stress over a wide area, and secondary cracks in the TR system were likely to form at defects located in the latewood layer away from the primary crack plane. These findings imply that the latewood layer may be subjected to intensive stress under tensile load and may be the initiation site of cracks.

Second, stable check propagation toward the pith was observed, while propagation toward the bark had a tendency to halt at the boundary between earlywood and latewood (see white arrows in Fig. 8b,c). Then some of the checks approached in front of the latewood. When there is a secondary check aligned in the latewood ahead of the primary check tip, the two checks joined to become a longer check (see black arrows in Fig. 8c,d). In contrast, when there was no corresponding check in the forward latewood, the check was arrested and did not propagate further. This crack arrest is consistent with the difference in fracture toughness of the TR system within a single annual ring; a crack growing toward a stiffer material experiences reduced stress intensity, resulting in increased macroscopic fracture toughness of the material.[25] Therefore, as a crack approaches the stiffer latewood, crack tip shielding offers a possible mechanism for crack arrest. The experimental measurements and the numerical calculations of K_{IC} in the TR system as a function of crack tip position within a single annual ring strongly demonstrated this effect.[26,27]

Within the limitations of the sugi species, the results of the SEN bending tests can be summed up as follows: cracks perpendicular to the tangential direction initiate radially with ease, and then crack arrest occurs to prevent the cracks growing. This finding provides a consistent interpretation of the end-check propagation during drying which was experimentally observed. The mechanism of end-check propagation during drying cannot be directly explained by fracture mechanics. However, this study shows the relation between crack propagation based on fracture mechanics and end-check propagation during drying.

Assuming that the crack plane is semi-infinite normal to the two-dimensional surface, the fracture toughness of air-dried specimens was measured by SEN bending tests in this study. The plane of end checks, however, is finite and forms a closed system. As future work, it is suggested that end-check propagation in three dimensions should be analyzed. Also, more data on fracture toughness with different species and various moisture contents may contribute to the further evaluation of end-check propagation.

Conclusions

The mode I fracture toughness of air-dried sugi specimens in TR, TL, and intermediate systems, which correspond to the direction of end-check propagation, was examined by single-edge-notched bending tests. Then the occurrence and propagation of end checks in sugi (*Cryptomeria japonica* D. Don) blocks during drying, as an analog to TR cracks, was observed at the scale of the annual rings.

The critical stress intensity factor (K_{IC}) decreased as the crack propagation direction changed from TL to TR. The

K_{IC} value in the TR system was significantly lower than that in the TL system. The area under the load–COD curve (which is a measure of fracture energy) in the TR system was more than twice those in the TL and intermediate systems. As the results revealed, cracks perpendicular to the tangential direction initiate radially with ease, and then crack arrest occurs to prevent growing. This finding provides a consistent interpretation of the end-check propagation observed during drying as follows.

At the first stage of drying, tiny checks form easily and selectively in the latewood or transition wood, and then steadily propagate toward the pith, whereas propagation toward the bark halts at the boundary between earlywood and latewood. Checks are arrested after approaching the latewood. When there is a secondary check aligned in the latewood ahead of the primary crack tip, the two checks join to form a longer check.

Although the mechanism of end-check propagation during drying cannot be directly explained by fracture mechanics, this study showed the relation between crack propagation based on fracture mechanics and end-check propagation during drying.

References

1. Simpson W (1999) Drying and control of moisture content and dimensional changes. In: Wood handbook: wood as an engineering material. General Technical Report FPL-GTR-113, US Department of Agriculture (USDA), Forest Service, Forest Products Laboratory, Madison
2. Murmanis L, River BH, Stewart H (1983) Microscopy of abrasive-planed and knife-planed surfaces in wood-adhesive bonds. Wood Fiber Sci 15:102–115
3. Stehr M, Seltman J, Johansson I (1999) Laser ablation of machined wood surfaces. 1. Effect on end-grain gluing of pine (*Pinus silvestris* L.) and spruce (*Picea abies* Karst.). Holzforschung 53:93–103
4. Stehr M, Johansson I (2000) Weak boundary layers on wood surfaces. J Adhesion Sci Technol 14:1211–1224
5. Stehr M, Östlund S (2000) An investigation of the crack tendency on wood surfaces after different machining operations. Holzforschung 54:427–436
6. Schniewind AP, Ohgama T, Aoki T, Yamada T (1982) Effect of specific gravity, moisture content, and temperature on fracture toughness of wood. Wood Sci 15:101–109
7. Petterson RW, Bodig J (1983) Prediction of fracture toughness of conifers. Wood Fiber Sci 15:302–316
8. Sobue N, Asano A (1987) Effects of loading speed and moisture content on crack propagation in the radial direction of wood. Mokuzai Gakkaishi 33:7–11
9. Reiterer A, Tschegg S (2002) The influence of moisture content on the mode I fracture behavior of spruce wood. J Mater Sci 37:4487–4491
10. Fujimoto N, Goto K, Mataki Y (1999) Fracture toughness of the surface layer of the boxed-heart square timber of Sugi associated with drying checks (in Japanese). Zairyo 48:223–228
11. Reiterer A (2001) The influence of temperature on the mode I fracture behavior of wood. J Mater Sci Lett 20:1905–1907
12. Sobue N, Bajolet D, Pluvinage G (1985) Effect of drying stress on the fracture toughness of wood. Mokuzai Gakkaishi 31:528–531
13. Okamura H (1976) Introduction to linear fracture mechanics (in Japanese). Baihukan, Tokyo
14. Walsh PF (1972) Linear fracture mechanics in orthotropic materials. Eng Fract Mech 4:533–541
15. Valentin G, Adjanohoun G (1992) Applicability of classical isotropic fracture mechanics specimens to wood crack propagation studies. Mater Struct 25:3–13
16. Thuvander F, Berglund LA (2000) In situ observations of fracture mechanisms for radial cracks in wood. J Mater Sci 35:6277–6283
17. Schniewind AP, Centeno JC (1973) Fracture toughness and duration of load factor I. Six principal systems of crack propagation and the duration factor for cracks propagating parallel to grain. Wood Fiber 5:152–159
18. Schniewind AP, Quarles SL, Lee S-H (1996) Wood fracture, acoustic emission, and the drying process, part 1. Acoustic emission associated with fracture. Wood Sci Technol 30:273–281
19. Fonselius M, Riipola M (1992) Determination of fracture toughness of wood, J Struct Eng 118:1727–1740
20. King MJ, Sutherland IJ, Le-Ngoc L (1999) Fracture toughness of wet and dry *Pinus radiata*. Holz als Roh- und Werkst 57:235–240
21. Maruyama N, Okazaki H (1981) Cleavage fracture toughness of wood: Effects of annual ring angle on crack propagation (in Japanese). Bull Fac Agric Shizuoka 31:33–39
22. Harmuth H, Rieder K, Krobath M, Tschegg EK (1996) Investigation of the nonlinear fracture behavior of ordinary ceramic refractory materials. Mater Sci Eng A214:53–61
23. Stanzl-Tschegg SE (2009) Fracture properties of wood and wood composites. Adv Eng Mater 11:600–606
24. Hillerborg A (1991) Application of the fictitious crack model to different types of materials. Int J Fract 51:95–102
25. Thuvander F, Jernkvist LO, Gunnars J (2000) Influence of repetitive stiffness variation on crack growth behavior in wood. J Mater Sci 35:6259–6266
26. Ando K, Sato K, Fushitani M (1991) Fracture toughness and acoustic emission characteristics of wood I. Effects of the location of a crack tip in an annual ring (in Japanese). Mokuzai Gakkaishi 37:1129–1134
27. Ando K, Ohta M (1999) Variability of fracture toughness by the crack tip position in an annual ring of coniferous wood. J Wood Sci 45:275–283